

Supporting Information for the manuscript

A mesoporous lanthanide-organic framework constructed from a dendritic hexacarboxylate with cages of 2.4 nm

Yabing He,^a Hiroyasu Furukawa,^b Chuande Wu,^c Mike O'Keeffe^d and Banglin Chen^{*b}

^a College of Chemistry and Life Sciences, Zhejiang Normal University, Jinhua 321004, China

^b Department of Chemistry, University of California and Molecular Foundry, Materials Sciences Division, Lawrence Berkeley National Laboratory, Berkeley, California 94720, USA

^c Department of Chemistry, Zhejiang University, Hangzhou 310027, China

^d Department of Chemistry and Biochemistry, Arizona State University, Tempe, Arizona 85287, USA

^e Department of Chemistry, University of Texas at San Antonio, One UTSA Circle, San Antonio, Texas 78249-0698, USA. Fax: (+1)-210-458-7428; E-mail: banglin.chen@utsa.edu

General remarks

All starting materials and reagents for synthesis were commercially available and used as received. Fourier transform infrared (FTIR) spectra were recorded using a Bruke Vector 22 spectrometer between 650 cm^{-1} and 4000 cm^{-1} . Thermogravimetric analyses (TGA) were carried out using a Shimadzu TGA-50 thermal analyzer with a heating rate of 5 $^{\circ}\text{C min}^{-1}$ in a flowing nitrogen atmosphere. Powder X-ray diffraction (PXRD) patterns were recorded on a Rigaku Ultima IV X-ray diffractometer operating at 40 kV and 44 mA with a scan rate of 1.0 deg min^{-1} , using $\text{Cu-K}\alpha$ radiation. Low-pressure gas adsorption experiments were carried out on a Quantachrome AUTOSORB-1 automatic volumetric gas adsorption analyzer. Before the gas sorption measurements were performed, the as-synthesized samples were guest-exchanged with dry methanol, and then activated using supercritical CO_2 drying method to remove all solvent molecules. Briefly, the methanol-containing sample was placed in the chamber in a Tousimis Samdri PVT-3D critical point dryer, and methanol was completely exchanged with liquid CO_2 . The CO_2 was slowly vented from the chamber, yielding the activated material **UTSA-61a**.

Single-crystal X-ray crystallography

The crystal data were collected on an Oxford Xcalibur Gemini Ultra diffractometer with an Atlas detector. The data were collected using graphite-monochromated $\text{Mo K}\alpha$ radiation ($\lambda = 0.71073 \text{ \AA}$) at 293 K. The datasets were corrected by empirical absorption correction using spherical harmonics, implemented in the SCALE3 ABSPACK scaling algorithm. The structure was solved by direct methods and refined by full matrix least-squares methods with the SHELX-97 program package. Because of the poor crystal quality and the highly disordered Me_2NH_2^+ cations and DMA molecules in the compound, the SQUEEZE subroutine of the PLATON software suit was used to remove the scattering from the highly disordered guest molecules. The resulting new files were used to further refine the structures. However, distortion still exists for the ligand, especially the Uij values of some atoms. These results suggest

that the distortion is from the inherent nature of the crystals. The H atoms on C atoms were generated geometrically. All atoms are refined anisotropically.

Synthesis and characterization of UTSA-61

A mixture of the organic building block H₆L (10.0 mg, 9.7 μmol) and Tb(NO₃)₃·6H₂O (25.0 mg, 55.2 μmol, Aldrich) was dispersed in *N,N'*-dimethylacetamide (DMA, 1.5 mL) in a disposable scintillation vial (20 mL) under sonication. The vial was capped and heated at 90 °C for 72 h. The block-shaped crystals were collected in 44% yield. FTIR (neat, cm⁻¹): 1608, 1583, 1508, 1394, 1261, 1186, 1014, 860, 787, 708.

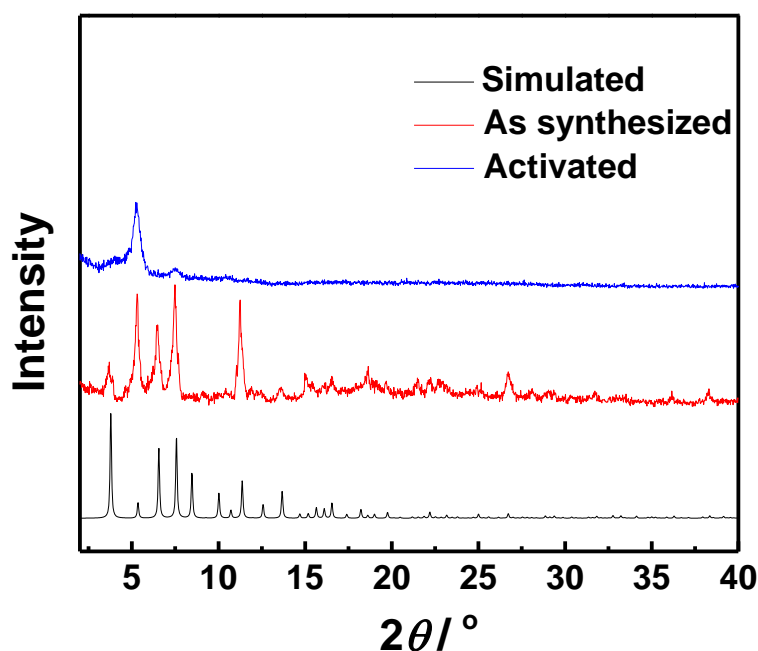


Figure S1. PXRD patterns of as-synthesized **UTSA-61** (red) and activated **UTSA-61a** (blue), along with the simulated XRD pattern from the single-crystal structure (black).

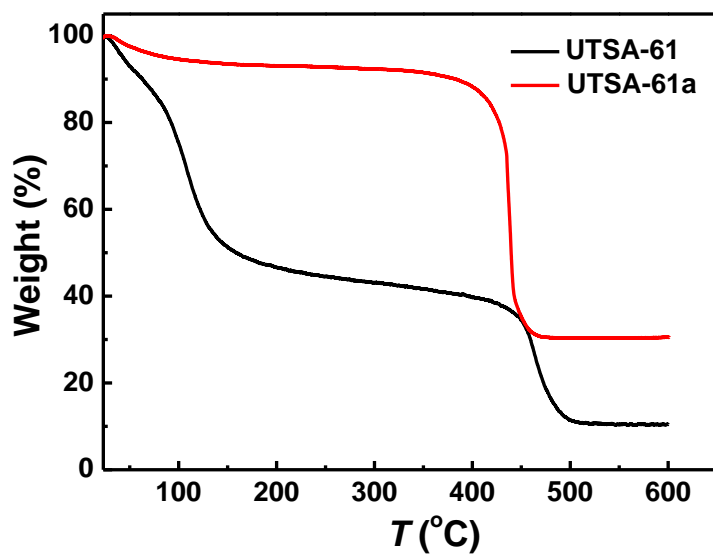
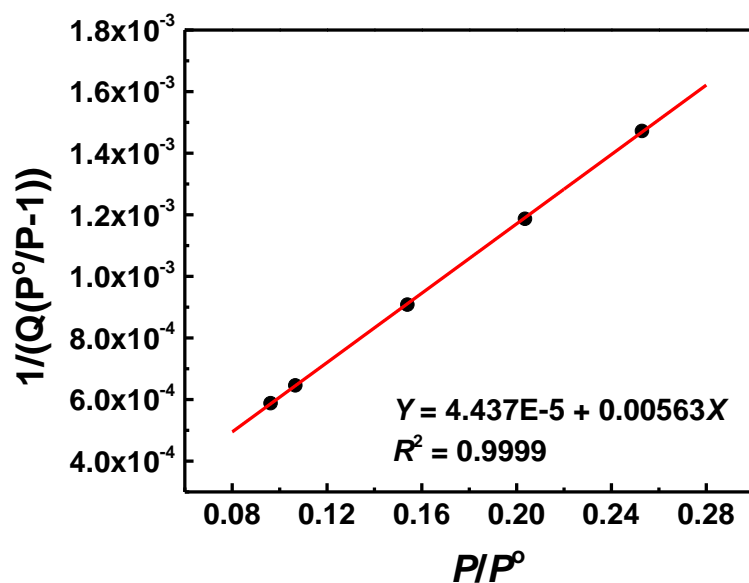


Figure S2. TGA curves of **UTSA-61** (black) and **UTSA-61a** (red) at a heating rate of 5 °C/min under a flowing N₂ atmosphere.



$$S_{\text{BET}} = (1/(0.00563 + 0.00004437))/22414 \times 6.023 \times 10^{23} \times 0.162 \times 10^{-18} = 767 \text{ m}^2/\text{g}$$

Figure S3. BET plot of **UTSA-61a**. Only the range below $P/P_0 = 0.26$ satisfies the first consistency criterion for applying the BET theory.

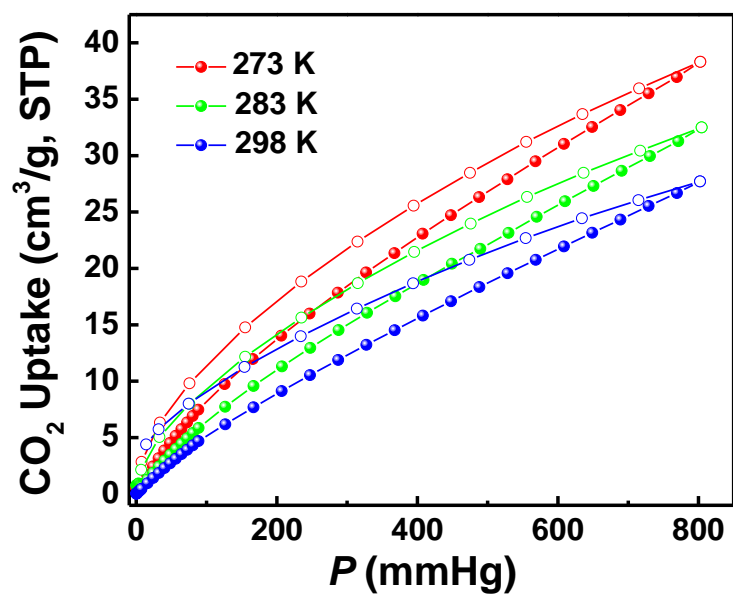


Figure S4. CO₂ sorption isotherms of UTSA-61a at 273 K (red), 283 K (green) and 298 K (blue). Filled and open symbols represent adsorption and desorption data, respectively. The solid lines were used to guide the eye.

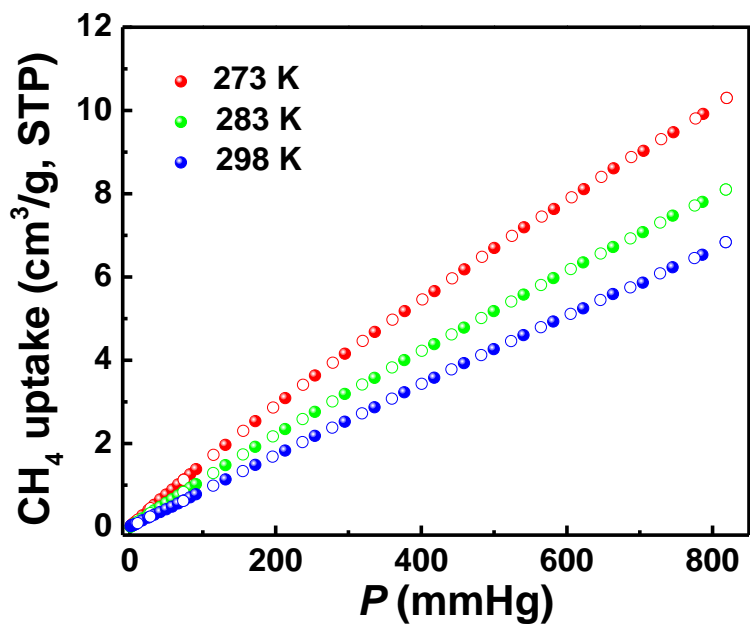


Figure S5. CH₄ sorption isotherms of UTSA-61a at 273 K (red), 283 K (green) and 298 K (blue). Filled and open symbols represent adsorption and desorption data, respectively.

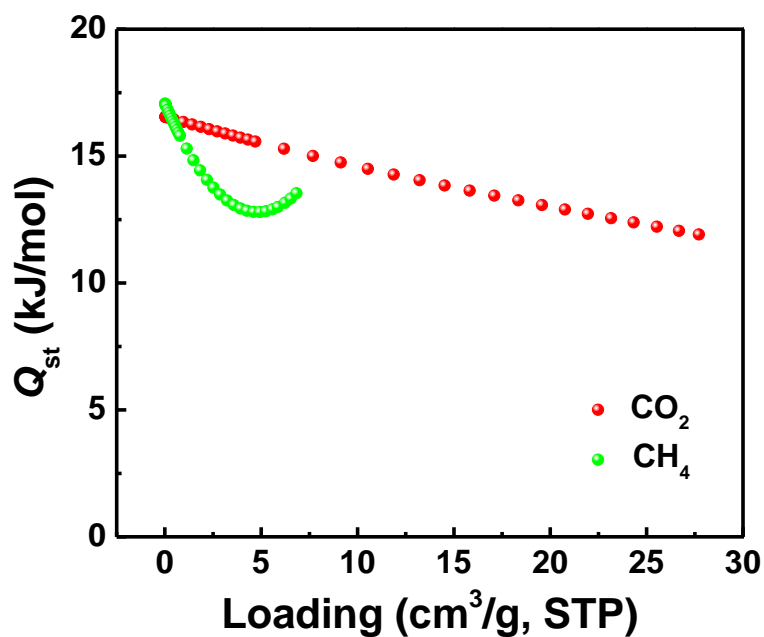


Figure S6. The isosteric heat of CO₂ (red) and CH₄ (green) adsorption in **UTSA-61a**.

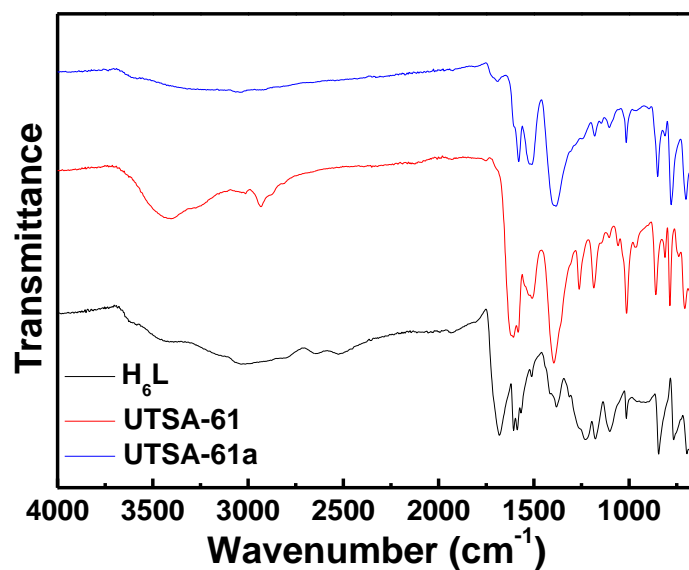


Figure S7. FTIR spectra of the organic linker H₆L (black), as-synthesized **UTSA-61** (red) and activated **UTSA-61a** (blue).